HAL
archives-ouvertes.fr

PB 6378 and PB 9261: Two new systems of interacting galaxies with starbursts

C. Vanderriest, Henri Reboul

▶ To cite this version:

C. Vanderriest, Henri Reboul. PB 6378 and PB 9261: Two new systems of interacting galaxies with starbursts. Astronomy and Astrophysics Supplement Series, EDP Sciences, 1991, 251 (1), pp.43-48. hal-02160130

HAL Id: hal-02160130
https://hal.archives-ouvertes.fr/hal-02160130

Submitted on 19 Jun 2019

HAL is a multi-disciplinary open access archive for the deposit and dissemination of scientific research documents, whether they are published or not. The documents may come from teaching and research institutions in France or abroad, or from public or private research centers.

L'archive ouverte pluridisciplinaire **HAL**, est destinée au dépôt et à la diffusion de documents scientifiques de niveau recherche, publiés ou non, émanant des établissements d'enseignement et de recherche français ou étrangers, des laboratoires publics ou privés.

1991A&A...251...43V

Astron. Astrophys. 251, 43–48 (1991)

ASTRONOMY AND ASTROPHYSICS

PB 6378 and PB 9261: Two new systems of interacting galaxies with starbursts ⋆

C. Vanderriest [1] **and H. Reboul** [2]

[1] Observatoire de Paris-Meudon (DAEC) et URA 173 du CNRS, 5 place Janssen, F-92195 Meudon Cedex, France
[2] Laboratoire d'Astronomie, Université Montpellier II et URA 1368 du CNRS, F-34095 Montpellier Cedex 5, France

Received December 7, 1990; accepted May 13, 1991

Abstract. Extracted from the Berger-Fringant catalogue of faint blue objects, PB 6378 and PB 9261 are two systems of interacting galaxies with prominent starbursts. Photometry of these systems was done by electronography; bidimensional spectroscopic data with spatial resolution $\leqq 1''$ were obtained by using a fibre optics spectrograph.

Spectra integrated over the different components are then obtained, as well as velocity fields and intensity maps in the continuum and in the emission lines. This allows to estimate the physical conditions in these starburst systems. We discuss the interest of extending the method to similar but more distant objects.

Key words: galaxies: active – kinematics and dynamics – observational method – image processing – galaxies: PB 6378 – PB 9261

1. Introduction

A systematic search for distant multiple AGNs (active galaxy nuclei), possibly including gravitational mirages or true binary quasars could be useful for several purposes. Gravitational mirages now have several well-known astronomical applications while physical pairs of quasars could be a way towards an unbiased estimation of q_0 (Reboul et al. 1985).

An effective method of detection is to operate a double screening, first by colour and then by morphology. We plan to conduct such a survey by an automatic reduction of Schmidt plates in several colours developped for the MAMA microdensitometer (Berger et al. 1991). However, in a first step, we looked for candidates among existing catalogues of UV-excess objects that, put together, cover about 3000 square degrees and total about $2\ 10^4$ objects selected among $2\ 10^6$. In the subset of these colour selected objects, we found ~ 70 pairs or possible pairs with separation less than $10''$. Among the 23 candidates observed up to now, one is a possible double quasar (Reboul et al. 1987), and 10 are extragalactic systems, including 8 pairs of strongly interacting galaxies with starburst or Seyfert nuclei.

We will use the neologism "*interactivating*" for such pairs in which the gravitational interaction presumably is the *primum movens* of strong nuclear starburst or AGN activity through complex dissipative processes. Pairs of starburst galaxies are an interesting by-product of the selection process: they are possible progenitors of pairs of AGNs as well as the privileged loci to study the cosmological evolution of the starburst phenomenon. Moreover, *interactivation* may act as a tracer for otherwise low surface brightness galaxies, thus permitting to complete the study of their space distribution at larger redshifts (Thuan et al. 1991).

The IRAS survey has also revealed a surprisingly large population of starburst systems at low redshifts (see for instance Lawrence et al. 1989). The two low-redshift ($z < 0.1$) pairs that will be discussed here are not listed as infrared sources but could be detected up to $z \simeq 0.5$ with our optical method. Integral field spectrophotometry seemed the best way to get information on them, since it allows an optimal separation of the stellar population and emitting gas components.

2. Observations and data analysis

PB 6378, noted as compact in the Berger-Fringant catalogue (Berger & Fringant 1980), appears clearly double on the POSS-O print, while PB 9261 (Berger & Fringant 1984) is noted as *compact object or close binary with 2 blue components, separation* $\leqq 2''$. In fact, for both systems, complex structures appear on higher resolution pictures obtained with a valve electronographic camera (Baudrand et al. 1982) mounted at the prime focus of the Canada-France-Hawaii telescope (CFHT). Bidimensional spectrographic data were obtained later with the SILFID spectrograph (Vanderriest & Lemonnier 1988) at the Cassegrain focus of the CFHT.

2.1. Observation material

The journal of observations is given in Table 1. In imaging mode, the spatial sampling of the electronographic camera (E.C.) corresponds to the 20 μm pixels of digitized images. In spectrographic mode, the spatial sampling in the focal plane is fixed by the size of the 100 μm fibres whose monochromatic images are 60 μm wide on the detector. For the 1986 data, this was an electrostatically focused photon counting camera (P.C.C.) described elsewhere (Hua et al. 1987). This detector had only 256×256 pixels whose size was adjusted at its practical minimum value of 36 μm.

Send offprint requests to: H. Reboul

⋆ Based on observations made at the Canada-France-Hawaii telescope (Hawaii)

© European Southern Observatory • Provided by the NASA Astrophysics Data System

1991A&A...251...43V

Table 1. Journal of observations

Object	Instrument	Detector	Date	Exposure (mn)	Wavelength range (Å)	Dispersion (Å/mm)	Seeing (″)	Sampling (″)
PB 6378	Imaging	E.C.	16/10/82	10	*V* filter		0.75	0.15
PB 6378	Imaging	E.C.	16/10/82	10	*B* filter		0.80	0.15
PB 6378	Imaging	E.C.	16/10/82	10	*U* filter		0.90	0.15
PB 6378	Imaging	E.C.	09/10/83	30	*U* filter		0.90	0.15
PB 6378	SILFID	P.C.C.	04/12/86	30	6300–7180	100	1.1	0.71
PB 6378	SILFID	P.C.C.	04/12/86	45	4950–5800	100	1.1	0.71
PB 6378	SILFID	C.C.D.	05/12/88	30	4690–5940	100	1.2	0.71
PB 9261	Imaging	E.C.	17/10/82	10	*V* filter		0.82	0.15
PB 9261	Imaging	E.C.	17/10/82	10	*B* filter		0.85	0.15
PB 9261	Imaging	E.C.	17/10/82	15	*U* filter		0.90	0.15
PB 9261	SILFID	P.C.C.	04/12/86	40	6300–7180	100	1.2	0.71
PB 9261	SILFID	P.C.C.	04/12/86	20	4950–5800	100	1.2	0.71
PB 9261	SILFID	P.C.C.	04/12/86	15	4620–6700	235	1.2	0.71

For the 1988 data, the detector was a Thomson CCD, with 576×384 pixels of 23 μm, giving a better sampling of the fibre images.

2.2. *Data reduction*

The photometric reduction of the electronographic plates was done in the usual manner (see Baudrand et al. 1982).

In its "Integral Field Spectroscopy" mode, SILFID makes use of a compact fibre optics device for transforming the bidimensional field of view into an entrance "slit". The possibilities of this system and the details of data reduction are discussed in previous papers (Angonin et al. 1990; Malivoir et al. 1990; Haddad & Vanderriest 1991). An important step of the process is the image reconstitution in preselected continuum bands and emission lines; this allows to define the regions in which spectra of individual fibres can be safely coadded. Unfortunately the size of the detectors available at the time of observation did not allow to cover more than 1/3 of the total "slit" length, thus limiting the field of view in the same proportion.

3. Results on PB 6378

3.1. *Direct imaging*

Electronographic plates of the field in *U*, *B* and *V* colours were obtained in 1982 and 1983 under good seeing conditions (Fig. 1). The photometric calibration was performed by transfer, on short exposure plates, of a standard sequence in the nearby Selected Area 92 (Priser 1974) and the resulting stellar sequence around PB 6378 was extended to magnitudes $\simeq 22$ on longer exposures. Good photometry of the components of the system was thus possible (Table 2). The general morphology is suggestive of a strong tidal interaction. The main galaxy (thereafter PB 6378-A) looks disturbed with a bright nucleus and several condensations on the underlying disk; the companion (PB 6378-B) is resolved into 3 "knots" noted k1 to k3. A remarkable feature is the bridge that links A and B. It is quite blue ($B-V=0.35\pm0.15$; $U-B=-0.3\pm0.15$), bright and thin (width $<0.7''$, i.e. 1.5 kpc for a length of 17 kpc with $H_0=50, q_0=1/2$; *these values of* H_0 *and* q_0 *will be used thereafter for evaluating absolute quantities*). The absolute magnitudes listed in Table 2 have been calculated without considering the reddening nor the K-correction. In fact, the colour indices are about the same for all the observed features, as can be seen on an $(U-V)$ colour map (Fig. 2), with the possible exception of a regular gradient in PB 6378-B, from knot k1 (which is the bluer) to k3. The apparent structure near the nucleus of PB 6378-A in Fig. 2 is an artifact due to the poorer seeing on the U plate.

3.2. *Bidimensional spectrography*

Star HZ 4 (Oke 1974) was used as spectrophotometric standard for the 1986 data and star Feige 15 (Stone 1977) for the 1988 ones. The absolute fluxes derived from these independant calibrations are in very good agreement.

The spectra show a blue continuum without significant absorption line, but with unresolved (FWHM $<200\,\mathrm{km\,s^{-1}}$) emission lines extended over the main bodies and the bridge. Figures 3 and 4 display the reconstructed field in the continuum and [O III] emission with 2 different representations: tramed images showing the fibre pattern and smoothed images. For PB 6378-A, the continuum and emission light distributions are very similar while a difference is seen for the companion: the light distribution in the pure continuum is smooth, with a maximum between k1 and k2, but these knots show up distinctly in the emission line pictures. On the integrated spectra, the lines are relatively stronger in the companion than in the main galaxy; in this latter, the line/continuum ratio is quite identical for the nucleus and the underlying disk. The bridge clearly appears only in the [O III] images.

From the emission lines, we obtain the redshift $z=0.0875$, without significant difference (within an accuracy of $\pm 40\,\mathrm{km\,s^{-1}}$) in the whole system, which seems to be seen face-on.

3.3. *Discussion*

The projected separation between PB 6378-A and B is 17 kpc (7.8″) and their true relative velocity is probably small, as suggested by the presence of the "bridge". Such characteristics use to favour the mutual induction of starbursts in both components. Line intensities, integrated on different parts of the system, are summarized in Table 3. The observed line ratios clearly fall, in the

© European Southern Observatory • Provided by the NASA Astrophysics Data System

1991A&A...251...43V

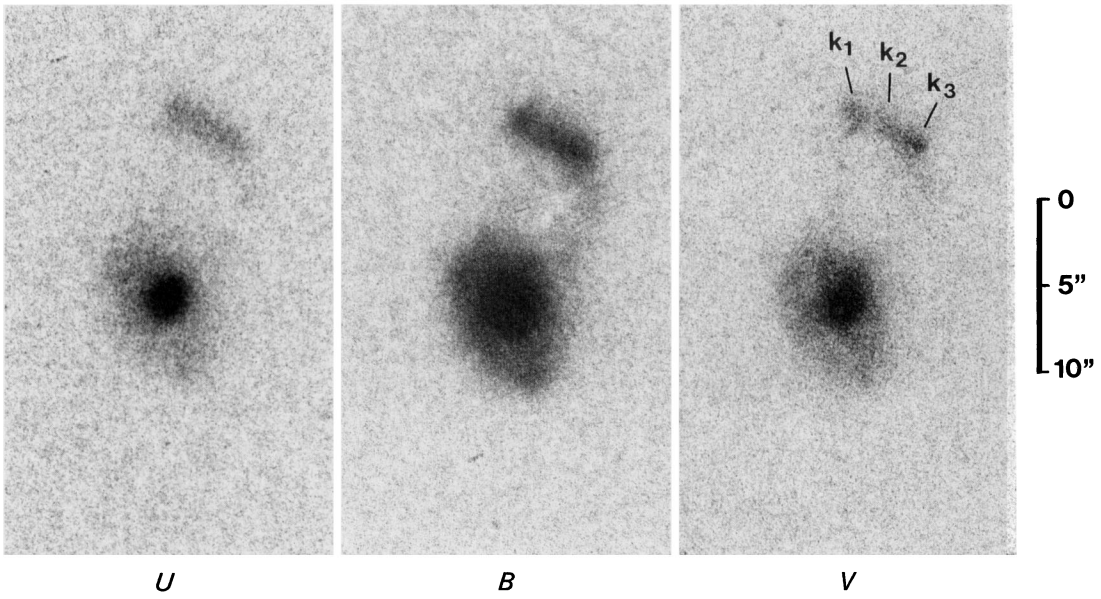

Fig. 1. Electronographic pictures of PB 6378 in U, B and V colours. Note the structures in the disk of PB 6378-A, the thin bridge, and the colour differences in the knots of PB 6378-B. North is up and East on the left

Table 2. Photometry of the PB 6378 system

Component	U	B	V	M_V (50, 1/2)
PB 6378A	16.60±0.03	16.75±0.03	16.55±0.03	−22.1
PB 6378B	18.19±0.04	18.55±0.04	18.22±0.04	−20.4
A: nucleus	18.14±0.05	18.17±0.05	18.03±0.05	−20.6
A: galaxy	16.90±0.04	17.09±0.04	16.87±0.04	−21.8
Bridge $A-B$	19.75±0.1	20.10±0.01	19.80±0.01	−18.8

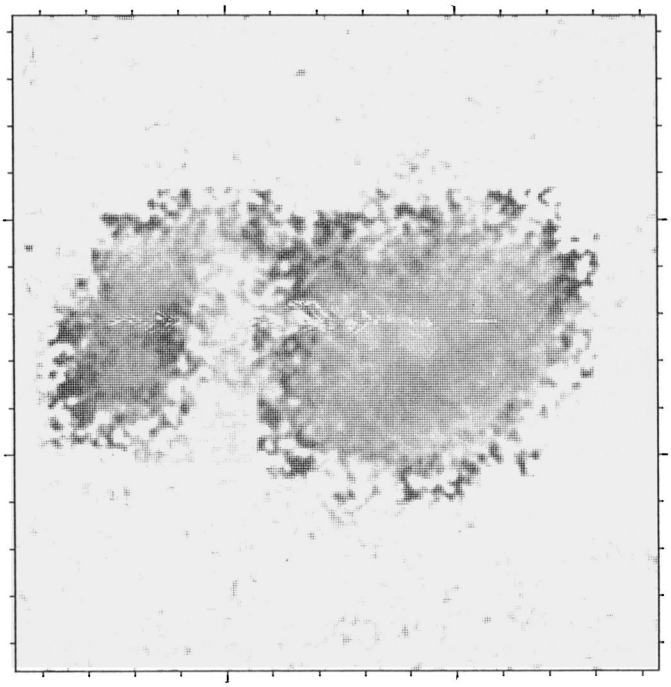

Fig. 2. $U-V$ colour map from the electronographic pictures of Fig. 1

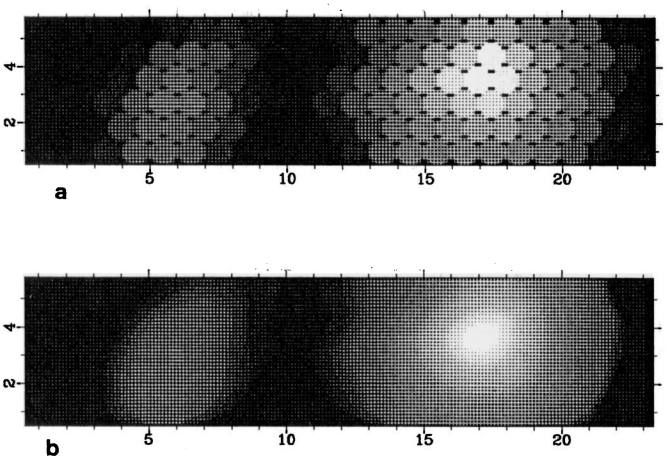

Fig. 3a and b. Reconstructed picture (shown in logarithmic gray scale) of the field of PB 6378 in continuum light ($\lambda \simeq 5300$ to 5700 Å), **a** direct reconstruction showing the fibre pattern. **b** After gaussian smoothing (FWHM ≃ 0.5 fibre)

© European Southern Observatory • Provided by the NASA Astrophysics Data System

1991A&A...251...43V

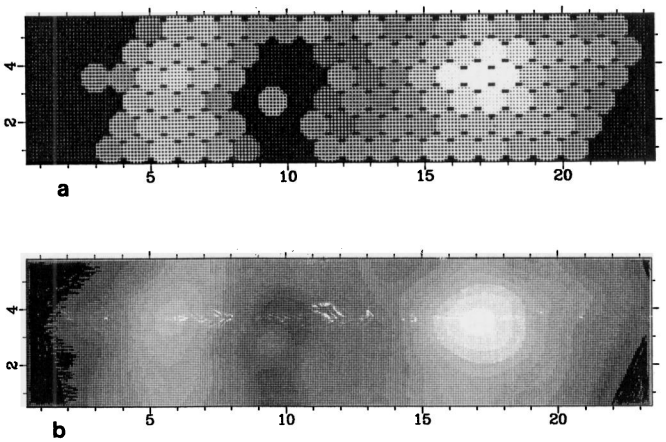

Fig. 4. As Fig. 3 but for the [O III] emission

diagrams of Veilleux & Osterbrock (1987), in the domain of H II regions or starburst galaxies and do not show any significant variation over the whole field, including the bright nucleus of PB 6378-A.

The locations in the $[O\,III]_{5007}/H\beta$ versus $[N\,II]_{6583}/H\alpha$ diagram agree with a model of photoionization by hot stars with effective temperature $T_* \simeq 4.3 \pm 0.1\ 10^4$ K, while the slightly higher temperature derived from $[O\,I]_{6300}$ suggests a marginal contribution of shocks to the heating of the emissive gas.

The galactic reddening is very faint in the direction of PB 6378; about $E(B-V) = 0.02$ from the maps of Burstein & Heiles (1982). The measured values of $H\alpha/H\beta$, compared with the expected one for a purely radiative excitation model, lead to internal extinctions at $H\beta$ of 0.6 ± 0.2 mag ($C_\beta = 0.24 \pm 0.08$) for PB 6378-A and 1.0 ± 0.3 mag ($C_\beta = 0.4 \pm 0.12$) for B. In fact, the real extinctions could be slightly lower if the emissions are superimposed to Balmer absorptions of the underlying stellar components, the value of the intensity being more affected for $H\beta$ than for $H\alpha$ (see for instance Leech et al. 1989). Spectra at shorter wavelengths would be necessary for judging the composition of the stellar population, and thus the magnitude of this effect.

The $H\beta$ flux, integrated on the whole system and dereddened, is about $20\ 10^{-18}$ W m^{-2}, corresponding to a luminosity $L(H\beta) \simeq 7\ 10^{34}$ W. Assuming a filling factor of 10^{-3} and an IMF in agreement with the observed T_* (Lequeux et al. 1981), this corresponds to a total mass of ionizing O-B stars $\simeq 5\ 10^7 M_\odot$. With $(M/L)_V = 1$ (typical of starburst galaxies), this is $\simeq 10^{-3}$ of the total mass of the system and probably also a small fraction of its total gas content. Nevertheless, depending on the duration of the burst, its evolution and on the shape of the IMF, the total mass of gas converted into new stars could be a factor 10–30 larger than estimated here. The fairly high concentration of the burst in the central region of component A (nearly half the emission luminosity is concentrated in an unresolved nucleus) suggests that it has evolved during at least 10^8 years.

4. Results on PB 9261

4.1. Direct imaging

On good resolution electronographic plates (Fig. 5), this very blue object is resolved into a main component and a long extension with a "condensation" in the middle. This morphology is quite unusual. The 2 most ressembling systems observed so far are the peculiar Seyfert galaxy Arp 151 ≡ Mrk 640 (Sargent 1970) and the galaxy GNB 15 (Lawrence et al. 1989).

No photometric calibration of our plates could be done; the magnitude of the system was obtained from the spectra (see below).

4.2. Bidimensional spectrography

Pictures in continuum light and gas emission (Fig. 6) show some differences. In the smooth light distribution of the stellar continuum, only two components can be identified: a main galaxy (A) and a diffuse component (B) at 4.1″. In [O III], the light distribution is more concentrated and B splits into 2 maxima located at 3.1″ (hereafter designated "condensation") and at 5.6″ (hereafter "companion") from the center of the main galaxy. Clearly, the appearance in direct imaging results from a mixing of these 2 distribution.

Table 3. Line intensities in PB 6378 (units are 10^{-18} W m^{-2})

Line:		Gal. A	Nucleus A	Gal. B	Bridge
	Integration area in $(")^2$	26.	4.	10.	2.4
$H\beta$		9.1 ± 0.4	4.1 ± 0.2	1.6 ± 0.2	0.09 ± 0.05
$[O\,III]_{4959}$		5.8 ± 0.3	2.9 ± 0.2	1.8 ± 0.2	0.35 ± 0.05
$[O\,III]_{5007}$		17.5 ± 0.8	9.0 ± 0.3	5.0 ± 0.3	1.1 ± 0.1
$He\,I_{5876}$		1.0 ± 0.3			
$[O\,I]_{6300}$		1.8 ± 0.3			
$[N\,II]_{6548}$		2.0 ± 0.3	0.5 ± 0.1		
$H\alpha$		31.0 ± 1.0	13.2 ± 0.4	6.2 ± 0.3	
$[N\,II]_{6583}$		6.8 ± 0.3	3.2 ± 0.2	0.5 ± 0.3	
$H\alpha/H\beta$		3.4 ± 0.2	3.2 ± 0.2	3.9 ± 0.4	
	$\langle Z \rangle$ [a]	$0.0875 \pm (1)$	$0.0875 \pm (1)$	$0.0875 \pm (1)$	$0.0875 \pm (1)$

Note:
[a] The number between parentheses concerns the last digit and represents internal error.

© European Southern Observatory • Provided by the NASA Astrophysics Data System

1991A&A...251...43V

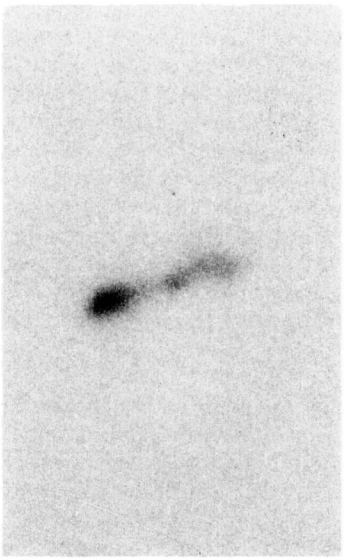

Fig. 5. Electronographic picture of PB 9261 in V filter. North is up and East on the left

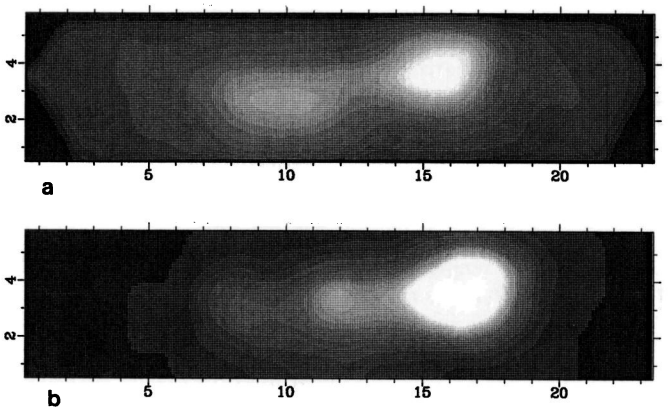

Fig. 6a and b. Reconstructed pictures (shown in linear gray scale) of the field of PB 9261 with gaussian smoothing (FWHM $\simeq 0.5$ fibre) **a** in continuum light ($\lambda \simeq 5400$ to 5800 Å) **b** in [O III] emission

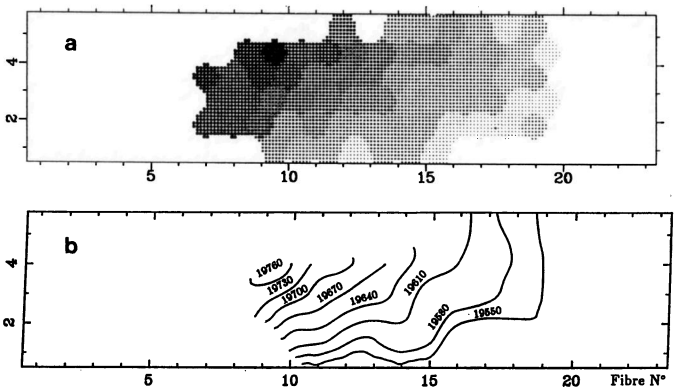

Fig. 7a and b. Velocity field in [O III] of PB 9261 displayed **a** in gray scale (white for $cz = 19\,500\,\mathrm{km\,s^{-1}}$, black for $cz = 19\,800\,\mathrm{km\,s^{-1}}$) and **b** as isovelocity contours

Integrated spectra show, as for PB 6378, a blue continuum and strong, unresolved (FWHM $< 200\,\mathrm{km\,s^{-1}}$) emission lines typical of starbursts, but the line/continuum ratio is higher. A well defined and regular velocity pattern can be traced from the emission lines (Fig. 7), compatible with a rotation motion around an axis tilted at $\simeq 25°$ on the major axis of the system.

We evaluated the V magnitude by integrating the continua of the object and the standard star (HZ 4) after multiplication by the response of a V filter. The total V magnitude of 17.3 ± 0.1 corresponds to $M_V \simeq -20.7$ given the mean redshift $z = 0.0657$.

Table 4. Line intensities in PB 9261 (units are $10^{-18}\,\mathrm{W\,m^{-2}}$)

Line:	Main component	Condensation	Companion
Integration area in $(")^2$	6.4	3.2	4.8
Hγ	4 ±0.5		
[O III]$_{4363}$	1 ±0.3		
Hβ	10 ±0.7	2.9±0.2	2.4±0.2
[O III]$_{4959}$	15 ±1	4.2±0.2	3.2±0.2
[O III]$_{5007}$	49 ±2	13.0±0.4	9.5±0.3
He I$_{5876}$	1.7±0.3		
[O I]$_{6300}$	0.6±0.2	0.3±0.1	0.7±0.1
Hα	33 ±1.5	12.1±0.4	8.3±0.3
[N II]$_{6583}$	1.8±0.3	0.3±0.1	0.7±0.2
He I$_{6678}$	0.6±0.3		
[S II]$_{6717}$	2.8±0.3	1.0±0.2	0.8±0.2
Hα/Hβ	3.3±0.3	4.2±0.3	3.5±0.3
$\langle Z \rangle$ [a]	0.06535±(5)	0.06570±(5)	0.06590±(5)

Note:
[a] The number between parentheses concerns the last digit and represents internal error.

© European Southern Observatory • Provided by the NASA Astrophysics Data System

1991A&A...251...43V

4.3. Discussion

From the data summarized in Table 4, we can infer classically the following physical parameters of the system:

– electronic temperature of the gas: 15000 ± 3000 K.

– electronic density: $n_e \leqq 10^3$ cm^{-3}.

– internal extinction (corrected for the very small galactic absorption) $\simeq 0.5$ magnitude at Hβ for the main galaxy and companion but $\simeq 1.3$ magnitude in the middle condensation.

– effective temperature of the excitating stars $T_* \simeq 4.5 \pm 0.1\ 10^4$ K. As noticed for PB 6378, we find an excess of intensity of $[O\,I]_{6300}$ with respect to a purely radiative excitation by stars at 45000 K, suggesting a possible contribution of shock in the excitation mechanism; this departure is especially noticeable for the companion.

– Hβ flux, integrated on the whole system and dereddened: $30\ 10^{-18}$ W m^{-2}, corresponding to a luminosity L (Hβ) $\simeq 6\ 10^{34}$ W. The total mass of ionizing O-B stars present in the burst, deduced from this luminosity with the usual assumptions, is again of the order of $5\ 10^7\ M_\odot$.

Considering the components A and B identified in continuum light as 2 colliding galaxies, their observed angular separation provides a lower limit for the impact parameter of the encounter. With our choices of H_0 and q_0, we get a projected separation of ~ 7.0 kpc. The difference of redshift between the barycenters of A and B gives a lower value for their true relative velocities: 100 ± 20 km s^{-1}. Assuming a parabolic encounter we thus calculate a lower limit for the total mass of the system: $8\ 10^9\ M_\odot$ and a mean M/L ratio $\geqq 0.5$. Considering the very blue shape of the continuum, a real value near this lower limit is not excluded. The PB 9261 system thus contains a relatively high percentage of very hot stars, of the order of 1% of the total mass. Depending on the exact shape of the mass fonction, and thus on the mean lifetime of the formed stars, the rate of star formation could be in the range $10-100\ M_\odot$ yr^{-1}, a considerable value for medium-sized galaxies.

5. Conclusions

PB 6378 and PB 9261 have been selected in the course of a survey aimed at finding multiple AGNs among faint blue objects, but they clearly are systems of interacting galaxies with vigorous starbursts. Their H_β luminosities approach, within a factor of 2, that of PG 0119 + 229 (≡ Mrk 357), one of the brightest classical starburst galaxies (Balzano 1983).

While PB 6378 is a bright disk galaxy interacting at low relative velocity with a smaller galaxy, the structure of the PB 9261 system is less clear; it could be 2 dwarf galaxies of nearly equal masses in close encounter or early phase of merging, inducing a powerful starburst.

A fair proportion of the objects selected as we did for PB 6378 and PB 9261 should be *interactivating* systems, either of the starburst or AGN types. By a systematic spectroscopic study, one can hope to find some having intermediate characteristics if, as is currently believed, an evolutionary link does exist between these 2 categories.

Starburst galaxies are generally strong I.R. emitters. The sensitivity of the IRAS survey allows to detect them only at low redshifts: A sharp cut-off clearly appears near $z = 0.04$ in the redshift distribution of an homogeneous sample of IRAS galaxies (Vader & Simon 1987). However, these 2 systems cannot have very high FIR luminosities. Their absence in the IRAS catalogue gives an upper limit $\simeq 2-3\ 10^{11}\ L_\odot$ and the FIR emission could be even fainter since both systems present only very modest internal extinction by dust. So our selection on purely optical criteria could reveal not only more distant cases than IR surveys but also objects with a different nature or in different states of interaction, thus broadening our views on the "*interactivation*" phenomenon.

Our attempt on this 2 low-z systems shows the feasibility of an extension of this work at cosmologically significant distances. For instance, at $z = 0.6$, a system like PB 6378 A, B would still appear as a pair of 20.5 and 22.1 V-magnitude objects separated by 2.7″ and could be studied in a reasonable time with the instrumentation we used on 4-m class telescopes.

Acknowledgements. It is a pleasure to express our gratefulness to A.M. Fringant who kindly brought us those two systems.

We would like to thank J. P. Picat for having obtained some of the electronographic plates and M. Caillat for his help with the EVE software. We thank also J. P. Lemonnier, for his efficient help during the observations with SILFID and J. M. Roques for the figures.

References

Angonin M.-C., Remy M., Surdej J., Vanderriest C., 1990, A&A 233, L5
Balzano V., 1983, ApJ 268, 602
Baudrand J., Chevillot A., Dupin J. P., Bellenger R., Félenbok P., Guérin J., Picat J. P., Vanderriest C., 1982, J. Optics Paris 13, 295
Berger J., Fringant A. M., 1980, A&AS 39, 39
Berger J., Fringant A. M., 1984, A&AS 58, 565
Berger J., Cordoni J. P., Fringant A. M., Guibert J., Moreau O., Reboul H., Vanderriest C., 1991, A&AS 87, 389
Burstein D., Heiles C., 1982, AJ 87, 1165
Haddad B., Vanderriest C., 1991, A&A 245, 423
Hua C. T., Grundseth B., Nguyen-Trong T., 1987, Astrophys. Lett. Commun. 25, 187
Lawrence A., Rowan-Robinson M., Leech K., Jones D., Wall J., 1989, MNRAS 240, 329
Leech K., Penston M., Terlevitch R., Lawrence A., Rowan-Robinson M., Crawford J., 1989, MNRAS 240, 349
Lequeux J., Maucherat-Joubert M., Deharveng J.-M., Kunth D., 1981, A&A 103, 305
Malivoir C., Encrenaz T., Vanderriest C., Lemonnier J.-P., Kohl-Moreira J.-L., 1990, Icarus 87, 412
Oke J., 1974, ApJS 27, 21
Priser J., 1974, Publ. U.S. Nav. Obs. Second Ser. XX, part 7
Reboul H., Fringant A. M., Vanderriest C., 1985, in: Proc. of the IAU symp. No 119, Bangalore. Reidel, Dordrecht, p. 547
Reboul H., Vanderriest C., Fringant A. M., Cayrel R., 1987, A&A 177, 337
Sargent W., 1970, ApJ 160, 405
Stone R., 1977, ApJ 218, 767
Thuan T.X., Alimi J.-M., Gott J.R., Schneider S.E., 1991, ApJ 370, 25
Vader J. P., Simon M., 1987, AJ 94, 854
Vanderriest C., Lemonnier J. P., 1988, in: Instrumentation for ground-based optical Astronomy. Proc. IXth Santa Cruz workshop, Robinson (ed.), Springer, Berlin Heidelberg New York, p. 304
Veilleux S., Osterbrock D., 1987, ApJS 63, 295

© European Southern Observatory • Provided by the NASA Astrophysics Data System